Microwave Magnetic-Envelope Dark Solitons in Yttrium Iron Garnet Thin Films

Ming Chen, Mincho A. Tsankov,[a] Jon M. Nash, and Carl E. Patton
Department of Physics, Colorado State University, Fort Collins, Colorado 80523
(Received 30 November 1992)

Dark solitons of magnetostatic surface waves in magnetic films have been observed for the first time. The experiments were conducted at 5.19 GHz on 7.2 μm single-crystal yttrium iron garnet films. The dark solitons were excited by 15 ns wide "off" pulses in a high power cw microwave signal applied to the film. The characteristic soliton narrowing effect in the output pulses was observed as the input power was increased above the 0.5–1 W threshold levels. The shape of the "dark" pulse agrees with the |tanh| functional dependence predicted from theory. Direct measurements of the carrier signal showed a phase shift of close to 180° at the center of the dark soliton, also in agreement with theory.

PACS numbers: 75.30.Ds, 76.50.+g, 85.70.Ge

Envelope solitons are nonlinear wave packets which preserve their shape without dispersive spreading. In recent years, soliton excitations have been realized in many physical systems [1–3]. One well-known example is the optical-envelope soliton in optical fibers [4,5]. Envelope solitons for spin waves at microwave frequencies have been observed in yttrium iron garnet (YIG) thin films for various magnetic field and propagation combinations, including forward-volume wave [6,7], surface wave [8], and backward-volume wave [9] configurations.

The envelope of nonlinear spin wave packets propagating in ferromagnetic thin films has been found to be best described by the nonlinear Schrödinger (NLS) equation [10,11]. It is well known that the NLS equation has two different types of solutions which correspond to bright and dark solitons, depending on the relative signs of the dispersion coefficient and the nonlinearity coefficient in the equation [12,13]. Bright soliton solutions exist when the product of these two coefficients is negative, while dark soliton solutions exist when the product is positive. All of the magnetic experiments to date have been for bright solitons, that is, for normal propagating wave packets.

This Letter reports the first observation of microwave magnetic-envelope dark solitons and the first experimental verification of the 180° phase shift in the carrier signal at the center of the pulse for any category of NLS dark soliton. The experiments were done at 5.19 GHz on in-plane magnetized single-crystal YIG films. Both the output signal envelope and the actual carrier signal output were measured. For input power levels above a certain threshold in the range of 0.5–1 W, the output signal pulses showed a narrowing which is characteristic of dark solitons and the carrier showed at 180° phase shift over the central minimum region, also characteristic of dark solitons. These results are in quantitative agreement with the theoretical dark soliton solutions for the NLS equation [13].

The propagating spin waves were excited in the magnetic thin film by applying cw microwave power to a magnetostatic wave (MSW) delay line structure using a microstrip transducer [14]. The width of the dark pulse was controlled by chopping the cw signal with a fast microwave switch. The cw signal was generated by a microwave synthesizer and a power amplifier, and controlled with a precision attenuator. The delay line structure utilized a single-crystal YIG film of 7.2 μm thickness on gadolinium gallium garnet substrate, 15 mm by 2 mm in size and with unpinned surface spins. The 10 GHz ferromagnetic resonance full linewidth of the film was 0.6 Oe. The film was magnetized by a static field of 1066 Oe applied in the film plane and perpendicular to the long 15 mm edge. This corresponds to the magnetostatic surface wave (MSSW) configuration. The input microstrip transducer was 50 μm wide and placed on the center portion of the film perpendicular to the long edge. The output signal was detected by a second identical microstrip transducer 4 mm down the film and analyzed with a Hewlett-Packard 71500A microwave transition analyzer. The operational frequency of 5.19 GHz and the static magnetic field of 1066 Oe were chosen to minimize transmission loss and keep the main lobe of the input pulse frequency spectrum within the MSSW bandwidth.

The experiment was conducted for various input power and pulse width combinations. The maximum input pulse power was 3 W and the minimum input dark pulse width was 5 ns. Best results were obtained for input dark pulses with width of 15 ns. Figure 1(a) shows output envelope signals for different dark pulse input power levels. At relatively low input power levels, as in panel (i), one sees only a broad output signal in a constant background. As the input power increased above some threshold, a sharp dark pulse emerges in the output signal and the width of the pulse is much narrower than the width of the input dark pulses. Trace (iv) has the expected dark soliton character, as discussed below. The voltage is near zero at the cusplike soliton center. It is important to note that such sharp output pulses occur only for dark pulse inputs. Output signals obtained under the same conditions as in Fig. 1(a), except that the input signals were regular "bright" pulses, are shown in Fig. 1(b). Only broad output signals are observed, even at high input power levels.

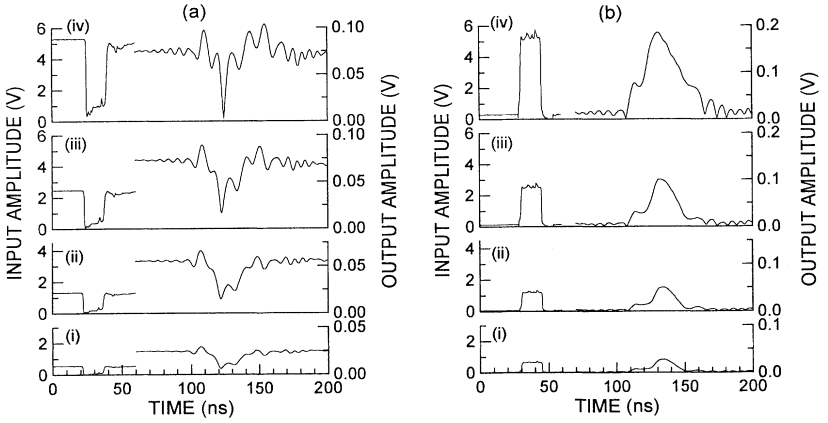

FIG. 1. (a) Series of output dark pulses for 15 ns wide input dark pulses with cw input power levels of (i) 7 mW, (ii) 30 mW, (iii) 130 mW, and (iv) 580 mW. (b) Output bright pulses for 15 ns wide input bright pulses at the same power levels as in (a).

In addition to measurements of the soliton envelope, it was also possible to measure the modulated microwave carrier signal directly. Figure 2 shows this 5.19 GHz carrier signal over a 2 ns time window at the soliton center, corresponding to the cusp in trace (iv) of Fig. 1(a). The dotted curve shows a pure sine wave at 5.19 GHz as a point of reference for phase. Figure 3 shows the actual phase change versus time data, represented by the solid circles, for the zero crossing points in the carrier signal at the center region of the soliton. The solid curve shows the phase change from theory, as discussed below.

The above results can be quantitatively explained on the basis of soliton theory. It can be shown [10,11] that the normalized envelope function for the classical complex spin wave precession amplitude $u(x,t)$ satisfies the nonlinear Schrödinger equation in the form

$$i\left(\frac{\partial u}{\partial t}+\omega_k'\frac{\partial u}{\partial x}\right)+\frac{1}{2}\omega_k''\frac{\partial^2 u}{\partial x^2}-N|u|^2u=0\,, \qquad (1)$$

where ω_k' and ω_k'' are the first- and the second-order partial derivatives of the spin wave frequency ω_k with respect to wave number k, respectively, and N is a nonlinearity coefficient defined by $N=\partial\omega_k/\partial|u|^2$. For simplicity, damping effects due to spin wave relaxation loss are not included in Eq. (1). Dark soliton solutions are possible when ω_k'' and N have the same sign; bright soliton solutions are possible when ω_k'' and N have opposite signs. For unpinned films in the MSSW configuration, the dispersion coefficient ω_k'' and the nonlinearity coefficient N are both negative (see, for example, [11]). The present experiment, therefore, corresponds to the dark soliton case. The expression for the dark soliton solution to Eq. (1) can be written as [13]

$$u(x,t)=\frac{(\omega_k''/N)^{1/2}}{v_g\tau_0}\left[\frac{(1-A^2)^{1/2}}{A}+i\tanh\left(\frac{t-t_0-x/v_g}{\tau_0}\right)\right]e^{i(\tilde{\kappa}x-\tilde{\Omega}t)}. \qquad (2)$$

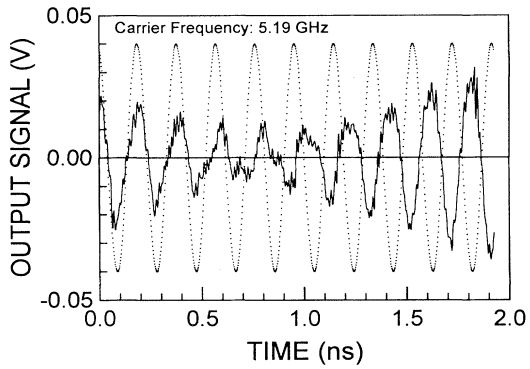

FIG. 2. Modulated microwave carrier signal at 5.19 GHz for a 2 ns window at soliton center, corresponding to the dark output pulse in Fig. 1(a), trace (iv).

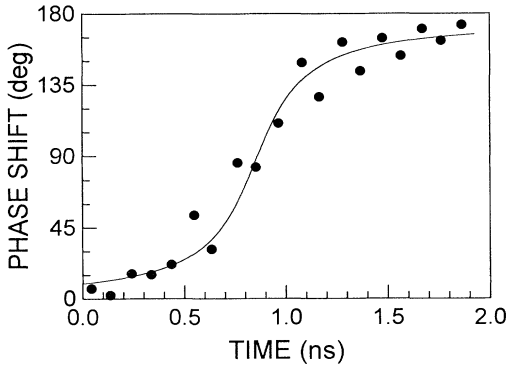

FIG. 3. Phase change vs time for the modulated microwave carrier signal in Fig. 2. The solid line shows a best fit of the theory described in text to the data.

The soliton group velocity v_g is given by

$$v_g = \omega_k' + \kappa\omega_k'' . \tag{3}$$

The $\tilde{\kappa}$ and $\tilde{\Omega}$ parameters in Eq. (2) are given by

$$\tilde{\kappa} = \kappa - \frac{(1-A^2)^{1/2}}{v_g \tau_0 A} \tag{4}$$

and

$$\tilde{\Omega} = \kappa\omega_k' + \frac{1}{2}\kappa^2\omega_k'' + \frac{\omega_k''(3-A^2)}{2v_g^2\tau_0^2 A^2} - \frac{(1-A^2)^{1/2}}{\tau_0 A} . \tag{5}$$

The κ and τ_0 parameters represent a soliton wave-number shift and the temporal half-width for the soliton pulse, respectively. The A parameter denotes the contrast of the dark soliton, with $-1 \le A \le 1$. Note that the complex phase term in Eq. (2) is not the spin wave carrier signal. It is part of the complex envelope function, with $\tilde{\kappa} \ll k$ and $\tilde{\Omega} \ll \omega_k$. From Eq. (2), the overall phase change in the soliton carrier in the soliton central region is given by

$$\sigma = \sin^{-1} A + \tan^{-1}\left[\frac{A}{(1-A^2)^{1/2}} \tanh\left(\frac{t - t_0 - x/v_g}{\tau_0}\right)\right] . \tag{6}$$

The dark soliton solution $u(x,t)$ in Eq. (2) for high contrast, that is, for $|A| \approx 1$, has two important and unique properties: (1) a |tanh| functional dependence for the envelope and a corresponding near-zero amplitude at soliton center; (2) a near-180° phase change from one side to the other across the soliton center. The |tanh| function in the envelope dark soliton solution causes the discontinuity in the slope of the dark soliton wave form at the soliton center and explains the sharp cusp in trace (iv) of Fig. 1(a). This cusp is a unique characteristic of dark solitons. When allowed, that is, for ω_k'' and N of opposite signs, the bright soliton solutions to Eq. (1) involve a sech function with a smooth profile at the center.

The sign change for the tanh function at dark soliton center is the origin of the observed close-to-180° phase change in the modulated carrier signal at the center of the MSSW dark soliton shown in Fig. 2. Equation (6) was used to obtain the theoretical phase shift versus time curve to compare with the data. The calculation was based on an estimate for the soliton half-width parameter from trace (iv) of Fig. 1(a) as $\tau_0 = 3.5$ ns, with $t_0 = 0.85$ ns and $x = 0$ to match the soliton center in Fig. 2. The key fitting parameter is the contrast parameter A, which affects strongly both the rate and the range of the phase change. The best fit to the data, shown by the solid line in Fig. 3, was obtained for $A = 0.9986$. Note that $A = 1$ would give a sharp step at the center of the soliton, not the gradual change shown in Fig. 3. The difference in the $A = 0.9986$ best fit value from unity is, therefore, significant. The excellent fit in Fig. 3 is further evidence for the dark soliton nature of the signals in Fig. 1(a). Experiments to date on optical dark solitons [5] had not been able to directly measure the phase shift due to the high carrier frequency of the optical pulses. In the case of microwave magnetic-envelope dark solitons, this phase shift has now been directly observed, measured, and fitted by theory.

In conclusion, this Letter reports on the first observation of microwave magnetic-envelope dark solitons in thin YIG films and the first direct measurement of the characteristic dark soliton 180° phase shift. Soliton theory, based on the nonlinear Schrödinger equation, is in quantitative agreement with the data.

Dr. B. A. Kalinikos of the St. Petersburg University of Electrical Engineering, St. Petersburg, Russia, is gratefully acknowledged for helpful discussions, advice, and assistance in establishing the microwave magnetic soliton program at Colorado State University. We would like to thank Dr. J. D. Adam of Westinghouse for providing the YIG films. We also thank Dr. M. J. Ablowitz, Dr. L. F. Mollenauer, and Dr. A. N. Slavin for helpful discussions. This work was supported in part by the National Science Foundation, Grant No. DMR-8921761 and by the U.S. Army Research Office, Grant No. DAAL03-91-G-0327.

[a]On leave of absence from Institute of Electrons, Bulgarian Academy of Sciences, Sofia, Bulgaria.

[1] M. J. Ablowitz and H. Segur, *Solitons and the Inverse Scattering Transformation* (SIAM, Philadelphia, 1981).

[2] G. L. Lamb, *Elements of Soliton Theory* (Wiley, New York, 1980).

[3] R. K. Dodd, J. C. Eilbeck, J. D. Gibbon, and H. C. Morris, *Solitons and Nonlinear Wave Equations* (Academic, London, 1982).

[4] L. F. Mollenauer, R. H. Stolen, and J. P. Gordon, Phys. Rev. Lett. **45**, 1095 (1980).

[5] P. Emplit, J. P. Hamaide, F. Reynaud, C. Froehly, and A. Barthelemy, Opt. Commun. **62**, 374 (1987); D. Krökel, N. J. Halas, G. Giuliani, and D. Grischkowsky, Phys. Rev. Lett. **60**, 29 (1988); A. M. Weiner, J. P. Heritage, R. J. Hawkins, R. N. Thurston, E. M. Kirschner, D. E. Leaird, and W. J. Tomlinson, Phys. Rev. Lett. **61**, 2445 (1988).

[6] B. A. Kalinikos, N. G. Kovshikov, and A. N. Slavin, Pis'ma Zh. Eksp. Teor. Fiz. **38**, 343 (1983) [JETP Lett. **38**, 413 (1983)].

[7] P. De Gasperis, R. Marcelli, and G. Miccoli, Phys. Rev. Lett. **59**, 481 (1987).

[8] B. A. Kalinikos, N. G. Kovshikov, P. A. Kolodin, and A. N. Slavin, Solid State Commun. **74**, 989 (1990).

[9] M. Chen, M. A. Tsankov, J. M. Nash, and C. E. Patton, in Abstracts Booklet of the 37th Annual Conference on Magnetism and Magnetic Materials, Houston, Texas, 1992, Abstract No. GE-02.

[10] V. P. Lukomskii, Ukr. Fiz. Zh. **23**, 134 (1978).

[11] A. K. Zvezdin and A. F. Popkov, Zh. Eksp. Teor. Fiz. **84**,

606 (1983) [Sov. Phys. JETP **57**, 350 (1983)].

[12] V. E. Zakharov and A. B. Shabat, Zh. Eksp. Teor. Fiz. **61**, 118 (1971) [Sov. Phys. JETP **34**, 62 (1972)]; *ibid.* **64**, 1627 (1973) [**37**, 823 (1973)].

[13] A. Hasegawa and F. Tappert, Appl. Phys. Lett. **23**, 142 (1973); *ibid.* **23**, 171 (1973); A. Hasegawa, *Optical Solitons in Fibers* (Springer-Verlag, Berlin, 1990), 2nd ed., p. 17.

[14] J. D. Adam, M. R. Daniel, P. R. Emtage, and S. H. Talisa, in *Physics of Thin Films*, edited by M. H. Francombe and J. L. Vossen (Academic, Boston, 1991), Vol. 15, p. 3, and references therein.